

A Halpern Method for Solving Perturbed Double Inertial Krasnoselskii–Mann Iterations with Applications to Image Restoration Problems



Rattanaporn Wangkeeree 1,4 , Rabian Wangkeeree 1,4 , Yirga Abebe Belay 1,2 , Kasamsuk Ungchittrakool 1,4,* , Purit Thammasiri 1 , Pakkapon Preechasilp 3

- ¹ Department of Mathematics, Faculty of Science, Naresuan University, Phitsanulok 65000, Thailand E-mails: rabianw@nu.ac.th; rattanapornw@nu.ac.th; kasamsuku@nu.ac.th; puritt64@nu.ac.th
- ² Department of Mathematics, Aksum University, P.O. Box 1010, Axum, Ethiopia E-mail: yirga2006@gmail.com
- ³ Department of Mathematics, Pibulsongkram Rajabhat University, Phitsanulok 65000, Thailand E-mail: preechasilpp@gmail.com
- ⁴ Center of Excellence in Mathematics, Faculty of Science, Naresuan University, Phitsanulok 65000, Thailand E-mails: rabianw@nu.ac.th; rattanapornw@nu.ac.th; kasamsuku@nu.ac.th

*Corresponding author.

Received: 5 June 2025 / Accepted: 30 August 2025

Abstract In this paper, we introduce and study a Halpern inertial method for solving the general perturbed Krasnoselskii–Mann type algorithm in Hilbert space settings, where the underlying mapping is quasi–nonexpansive. We discuss convergence analysis of the method under some mild assumptions on the control sequences. We additionally present a numerical example to demonstrate the effectiveness of the method. Finally, we apply the method in solving image restoration problems. We evaluate the quality of the Improvement in the Signal–to–Noise Ratio (ISNR) and the restored images using the Structural Similarity Index Measure (SSIM) metrics. The results of this work generalize and expand upon numerous results found in the literature.

 $\mathbf{MSC:}\ 47H09,\ 47H10,\ 47H14,\ 47J05,\ 47J25,\ 47J26$

Keywords: Fixed points; inertial iteration; perturbation parameters; quasi-nonexpansive mappings; strong convergence

Published online: 19 September 2025 © 2025 By TaCS-CoE, All rights reserve.



Published by Center of Excellence in Theoretical and Computational Science (TaCS-CoE)

1. Introduction

Given a real Hilbert space \mathbb{H} with inner product $\langle \cdot, \cdot \rangle$ and norm $\| \cdot \|$. Let $T \colon \mathbb{H} \to \mathbb{H}$ be any mapping. Then a point $p \in \mathbb{H}$ is said to be a fixed point of T if Tp = p. The set of all fixed points of T is denoted by F(T), that is, $F(T) = \{p : Tp = p\}$. The mapping T is said to be

i. nonexpansive if

$$||Tu - Tv|| \le ||u - v||$$
, for all $u, v \in \mathbb{H}$.

ii. quasi-nonexpansive if $F(T) \neq \emptyset$ and

$$||Tu - p|| \le ||u - p||$$
, for all $u \in H$, and $p \in F(T)$.

iii. monotone if

$$\langle Tu - Tv, u - v \rangle \ge 0$$
, for all $u, v \in \mathbb{H}$.

If T is multi-valued, then it is said to be monotone if

$$\langle \bar{u} - \bar{v}, u - v \rangle \ge 0$$
, for all $(u, \bar{u}), (v, \bar{v}) \in Graph(T)$,

where
$$Graph(T) = \{(u, v) \in \mathbb{H} \times \mathbb{H} : v \in Tu\}.$$

iv. maximally monotone if it is monotone and Graph(T) is not properly contained in the graph of any other monotone mapping.

Remark 1.1. It can be shown from (i) and (ii) that the class of nonexpansive mappings possessing a nonempty fixed point set is contained in the class of quasi-nonexpansive mappings.

Fixed point theory has got enormous applications across various domains ranging from pure and applied mathematics, economics, physics, engineering, computer science and others. Due to these and other applications, fixed point theory has attracted the interest of many researchers. Thus, several methods of approximating fixed points of different types of mappings have been introduced over the past years (see, for instance, [4, 23, 26, 38]). In particular, several iterative methods have been introduced to approximate fixed points of nonexpansive and quasi-nonexpansive mappings (see, for instance, [3, 8, 10, 11, 13, 16, 25, 28, 32–37, 40, 42, 44] and references therein).

One of the most famous and oldest fixed point iterations for nonexpansive mappings is the Krasnoselskii–Mann iteration which is given by the update

$$u_{n+1} = (1 - \lambda_n)u_n + \lambda_n T u_n, \tag{1.1}$$

where \mathbb{H} is a real Hilbert space and $T: \mathbb{H} \to \mathbb{H}$ is a nonexpansive mapping. The Krasnoselskii–Mann iteration was introduced independently by M. A. Krasnoselskii [15] and W. R. Mann [19]. They obtained weak convergence results under certain assumptions on the relaxation parameter λ_n . The Krasnoselskii–Mann iterations play a pivotal role in numerical variational analysis and optimization in which a number of real world problems can be modeled as fixed point problems. Moreover, these iterations have got several applications in convex optimization, signal and image processing, equilibrium problems and inverse problems. Consequently, many researchers have shown growing interest in Krasnoselskii–Mann iterations in recent years and several iterative methods have been proposed (see, for instance, [5–7, 9, 12, 14, 17, 21, 24, 31, 43] and references therein). Furthermore, numerous improvements have been made to the Krasnoselskii–Mann iteration process (see, for instance, [2, 5, 6, 9] and references therein).



In 2004, Combettes [6] considered the following inexact Krasnoselskii–Mann type algorithm

$$u_{n+1} = (1 - \lambda_n)u_n + \lambda_n(Tu_n + e_n), \tag{1.2}$$

where, $\{e_n\}$ represents an error occurring during the evaluation of Tu_n . He proved that the sequence $\{u_n\}$ generated by (1.2) converges weakly to a fixed point of a nonexpansive

mapping
$$T$$
, with $\{\lambda_n\} \subset (0,1)$ satisfying $\sum_{n=0}^{\infty} \lambda_n (1-\lambda_n) = \infty$ and $\sum_{n=0}^{\infty} \lambda_n ||e_n|| < \infty$.

In 2024, Maulen, Fierro and Peypouquet [20] introduced the following algorithm. Let $T_n : \mathbb{H} \to \mathbb{H}$ be a family of quasi-nonexpansive mappings with $\bigcap_{k \geq 1} F(T_k) \neq \emptyset$, for each $k \in \mathbb{N}$. They obtained a weak convergence of the sequence $\{u_n\}$ generated by

$$\begin{cases} v_n = u_n + \theta_n (u_n - u_{n-1}), \\ u_{n+1} = (1 - \lambda_n) v_n + \lambda_n T_n v_n. \end{cases}$$

And they also achieved a strong convergence result in the case that $\{T_n\}$ is a family of quasi-contractive mappings.

In 2023, Gebregiorgis and Kumam [9] proposed and studied the following inertial Mann–Halpern method to approximate fixed points. Let $C \subset \mathbb{H}$ be a nonempty, convex and closed, and $T: C \to \mathbb{H}$ be a nonexpansive mapping. Let $\{u_n\}$ be defined from arbitrary points $v, u_{-1}, u_0 \in C$ by

$$\begin{cases} v_n = u_n + \theta_n (u_n - u_{n-1}), \\ w_n = u_n + \phi_n (u_n - u_{n-1}), \\ z_n = (1 - \lambda_n) v_n + \lambda_n T w_n, \\ u_{n+1} = \alpha_n v + (1 - \alpha_n) z_n. \end{cases}$$
(1.3)

They proved that the sequence $\{u_n\}$ generated by (1.3) converges strongly to $p = P_{F(T)}v$, whenever $\{\theta_n\} \subset (0,1)$ and $\{\phi_n\} \subset [0,1)$ and $\{\lambda_n\}$ and the parameters $\{\alpha_n\}$ in (0,1) satisfy certain condition and $\lim_{n\to\infty} \frac{\theta_n}{\alpha_n} \left| \left| u_n - u_{n-1} \right| \right| = \lim_{n\to\infty} \frac{\phi_n}{\alpha_n} \left| \left| u_n - u_{n-1} \right| \right| = 0$.

Very recently, Cortild and Peypouquet [5] proposed and studied the following perturbed Krasnoselskii–Mann type iteration. Let \mathbb{H} be a real Hilbert space and let $T_n \colon \mathbb{H} \to \mathbb{H}$ be a family of quasi-contractive mappings. They obtained a strong convergence of sequence $\{u_n\}$ generated by

$$\begin{cases} v_n = u_n + \theta_n (u_n - u_{n-1}) + \epsilon_n, \\ w_n = u_n + \phi_n (u_n - u_{n-1}) + \rho_n, \\ u_{n+1} = (1 - \lambda_n) v_n + \lambda_n T_n w_n + \theta_n, \end{cases}$$

to the unique fixed point of T_n , provided that the inertial and relaxation parameters satisfy certain conditions and perturbation parameters $\epsilon_n, \rho_n, \theta_n \in l_1(\mathbb{H})$.

In light of these aforementioned findings, we pose the following important query.

Question 1.1. Is it possible to identify a technique for solving the inertial perturbed Krasnoselskii–Mann iteration with a more expansive category of mappings?

Inspired by the earlier mentioned results in the literature, especially by the results of [5] and [9], this paper presents and examines a Halpern type inertial method for approximating the perturbed Krasnoselskii–Mann iteration, where the underlying mapping is quasi-nonexpansive.

The following is how the rest part of the paper is structured. Section 2 deals with preliminary definitions, known properties of Hilbert spaces and some lemmas. In Section 3, we introduce our algorithm along with the detailed convergence analysis. In Section 4, we provide a numerical example to demonstrate the effectiveness of the algorithm. Some applications of our result on image restoration are given in Section 5, and Section 6 is devoted to some conclusions.

2. Preliminaries

Important lemmas and definitions that will be used in the sequel are covered in this section. In the remaining parts of the paper, the real Hilbert space will be represented by \mathbb{H} . The strong and weak convergence of a sequence $\{u_n\} \subset \mathbb{H}$ to a point u are denoted by $u_n \to u$ and $u_n \rightharpoonup u$, respectively.

The following basic relations are straight forward for all $u, v \in \mathbb{H}$:

$$||u+v||^2 \le ||u||^2 + 2\langle u+v,v\rangle$$
, and (2.1)

$$||u+v||^2 = ||u||^2 + 2\langle u, v \rangle + ||v||^2.$$
(2.2)

If for any sequence $\{u_n\} \subset \mathbb{H}$ and $u^* \in \mathbb{H}$, we have that $u_n \rightharpoonup u^*$ and $u_n - Tu_n \to 0$, as $n \to \infty$ implies that $Tu^* = u^*$, then we say that T satisfies the demiclosedness principle.

Let C be a nonempty, closed and convex subset of \mathbb{H} . The metric projection of a point $u \in \mathbb{H}$ onto C is the point, $P_C u$, of C satisfying

$$||P_C u - u|| = \inf \{||v - u|| : v \in C\}.$$

The metric projection mapping is nonexpansive and it exhibits the following basic property:

$$w = P_C u \iff \langle u - w, v - w \rangle \le 0, \text{ for all } v \in C.$$
 (2.3)

Lemma 2.1. [27] Let $\gamma, \sigma \in \mathbb{R}$. Then for all $u, v \in \mathbb{H}$, we have

$$\|\gamma u + \sigma v\|^2 = \gamma(\gamma + \sigma)\|u\|^2 + \sigma(\gamma + \sigma)\|v\|^2 - \gamma\sigma\|u - v\|^2.$$

Lemma 2.2. [18] Let $\{b_n\}$ be a sequence of nonnegative real numbers. If $\{b_{n_i}\}$ is a subsequence of $\{b_n\}$ such that $b_{n_i} < b_{n_i+1}$ for all $i \in \mathbb{N}$, then there exists an increasing sequence $\{m_k\}$ of natural numbers such that $\lim_{k\to\infty} m_k = \infty$ with the following properties for sufficiently large number $k \in \mathbb{N}$:

$$b_{m_k} \le b_{m_k+1} \quad and \quad b_k \le b_{m_k+1}.$$

Lemma 2.3. [39] Let $\{c_n\}$ be a sequence of nonnegative real numbers with

$$c_{n+1} \le (1 - \alpha_n) c_n + \alpha_n d_n,$$

where $\{\alpha_n\} \subset (0,1)$ such that $\sum_{n=1}^{\infty} \alpha_n = \infty$ and $\{d_n\}$ is a sequence of real numbers such that $\limsup_{n \to \infty} d_n \leq 0$, then $\lim_{n \to \infty} c_n = 0$.



Lemma 2.4. [22] Let $A: \mathbb{H} \to 2^{\mathbb{H}}$ be a maximally monotone mapping and $B: \mathbb{H} \to \mathbb{H}$ be any mapping. Define $T_r := (I + rA)^{-1}(I - rB)$, for r > 0. Then

$$F(T_r) = zer(A+B),$$

where $zer(A+B) = \{x \in \mathbb{H} \mid 0 \in (A+B)x\}.$

3. Main results

Here, we describe our algorithm and discuss its detailed convergence analysis. We are going to assume the following for the convergence analysis.

Conditions

- (C1) Let $T: \mathbb{H} \to \mathbb{H}$ be a quasi-nonexpansive mapping;
- (C2) Let $\{\alpha_n\} \subset (0,1)$ be such that $\lim_{n \to \infty} \alpha_n = 0$ and $\sum_{n=1}^{\infty} \alpha_n = \infty$;
- (C3) Let $\{\zeta_n\}$ be a sequence of positive numbers such that $\lim_{n\to\infty}\frac{\zeta_n}{\alpha_n}=0$;
- (C4) Let $\{\lambda_n\} \subset (0,1)$ with $\inf_n \lambda_n > 0$ and $\sup_n \lambda_n < 1$;
- (C5) Let ϵ_n , ρ_n , σ_n , η_n be in \mathbb{H} such that $\|\epsilon_n\| = o(\alpha_n)$, $\|\rho_n\| = o(\alpha_n)$, $\|\sigma_n\| = o(\alpha_n)$ and $\|\eta_n\| = o(\alpha_n)$.

We now state our proposed algorithm and discuss its convergence analysis.

Algorithm 3.1

Initialization: Let \bar{u} , u_0 , $u_1 \in \mathbb{H}$ and $\alpha \in [0,1)$. Set n=1. Then compute $\{u_n\}$ as follows:

Step 1: For the iterates $u_{n-1}, u_n \in \mathbb{H}$, choose θ_n and ϕ_n such that $0 \leq \theta_n \leq \delta_n$ and $0 \leq \phi_n \leq \delta_n$, where

$$\delta_n = \begin{cases} \min \left\{ \alpha, \frac{\zeta_n}{\|u_n - u_{n-1}\|} \right\}, & \text{if } \|u_n - u_{n-1}\| \neq 0, \\ \alpha, & \text{otherwise.} \end{cases}$$
 (3.1)

Step 2: Compute

$$\begin{cases}
v_n = u_n + \theta_n (u_n - u_{n-1}) + \epsilon_n, \\
w_n = u_n + \phi_n (u_n - u_{n-1}) + \rho_n, \\
z_n = (1 - \lambda_n)v_n + \lambda_n T w_n + \sigma_n, \\
u_{n+1} = \alpha_n \bar{u} + (1 - \alpha_n) T z_n + \eta_n.
\end{cases}$$
(3.2)

Remark 3.1. One can deduce from (3.1) and condition (C3) that

$$\lim_{n \to \infty} \frac{\theta_n}{\alpha_n} \left| \left| u_n - u_{n-1} \right| \right| = \lim_{n \to \infty} \frac{\phi_n}{\alpha_n} \left| \left| u_n - u_{n-1} \right| \right| = 0, \tag{3.3}$$

which in turn implies that

$$\lim_{n \to \infty} \theta_n \|u_n - u_{n-1}\| = \lim_{n \to \infty} \phi_n \|u_n - u_{n-1}\| = 0.$$
(3.4)

Theorem 3.2. If conditions (C1) - (C5) hold, then the sequence $\{u_n\}$ generated by Algorithm 3.1 is bounded.

Proof. Let $p \in F(T)$. Then we have from (3.2) and quasi-nonexpansiveness of T that

$$||u_{n+1} - p|| = ||\alpha_n \bar{u} + (1 - \alpha_n) T z_n + \eta_n - p||$$

$$= ||\alpha_n (\bar{u} - p) + (1 - \alpha_n) (T z_n - p) + \eta_n||$$

$$\leq \alpha_n ||\bar{u} - p|| + (1 - \alpha_n) ||T z_n - p|| + ||\eta_n||$$

$$\leq \alpha_n ||\bar{u} - p|| + (1 - \alpha_n) ||z_n - p|| + ||\eta_n||.$$
(3.5)

Since T is quasi-nonexpansive, it follows from (3.2) that

$$||z_{n} - p|| = ||(1 - \lambda_{n})v_{n} + \lambda_{n}Tw_{n} + \sigma_{n} - p||$$

$$\leq ||(1 - \lambda_{n})(v_{n} - p) + \lambda_{n}(Tw_{n} - p)|| + ||\sigma_{n}||$$

$$\leq (1 - \lambda_{n})||v_{n} - p|| + \lambda_{n}||w_{n} - p|| + ||\sigma_{n}||.$$
(3.6)

We also have from (3.2) that

$$||v_n - p|| = ||u_n + \theta_n(u_n - u_{n-1}) + \epsilon_n - p||$$

$$\leq ||u_n - p|| + \theta_n||u_n - u_{n-1}|| + ||\epsilon_n||.$$
(3.7)

Similarly, we obtain from (3.2) that

$$||w_n - p|| \le ||u_n - p|| + \phi_n ||u_n - u_{n-1}|| + ||\rho_n||.$$
(3.8)

Substituting (3.7) and (3.8) into (3.6), we obtain

$$||z_n - p|| \le (1 - \lambda_n) [||u_n - p|| + \theta_n ||u_n - u_{n-1}|| + ||\epsilon_n||] + \lambda_n [||u_n - p|| + \phi_n ||u_n - u_{n-1}|| + ||\rho_n||] + ||\sigma_n||.$$
(3.9)

Combining (3.9) and (3.5) results in

$$||u_{n+1} - p|| \le \alpha_n ||\bar{u} - p|| + (1 - \alpha_n) [(1 - \lambda_n) [||u_n - p|| + \theta_n ||u_n - u_{n-1}|| + ||\epsilon_n||]]$$

$$+ (1 - \alpha_n) [\lambda_n [||u_n - p|| + \phi_n ||u_n - u_{n-1}|| + ||\rho_n||]] + (1 - \alpha_n) ||\sigma_n||$$

$$\le \alpha_n ||\bar{u} - p|| + (1 - \alpha_n) ||u_n - p|| + \theta_n ||u_n - u_{n-1}|| + \phi_n ||u_n - u_{n-1}||$$

$$+ ||\epsilon_n|| + ||\rho_n|| + ||\sigma_n|| + ||\eta_n||.$$

(3.10)

Let us now denote

$$K = 7 \max \left\{ \|\bar{u} - p\|, \sup_{n \ge 1} \frac{\theta_n}{\alpha_n} \Big| \Big| u_n - u_{n-1} \Big| \Big|, \sup_{n \ge 1} \frac{\phi_n}{\alpha_n} \Big| \Big| u_n - u_{n-1} \Big| \Big|, \sup_{n \ge 1} \frac{\|\epsilon_n\|}{\alpha_n}, \sup_{n \ge 1} \frac{\|\rho_n\|}{\alpha_n}, \sup_{n \ge 1} \frac{\|\sigma_n\|}{\alpha_n}, \sup_{n \ge 1} \frac{\|\eta_n\|}{\alpha_n} \right\}.$$

With this notation, Inequality (3.10) simplifies to

$$||u_{n+1} - p|| \le (1 - \alpha_n) ||u_n - p|| + \alpha_n K$$

$$\le \max \{||u_n - p||, K\}\}$$

$$\vdots$$

$$\le \max \{||x_1 - p||, K\}.$$
(3.11)

Therefore, $\{u_n\}$ is bounded. Boundedness of $\{v_n\}$, $\{w_n\}$ and $\{z_n\}$ readily follows from the boundedness of $\{u_n\}$ and (3.2). This completes the proof our theorem.

Theorem 3.3. If conditions (C1) - (C5) hold, then the sequence $\{u_n\}$ generated by Algorithm 3.1 converges strongly to $p^* = P_{F(T)}\bar{u}$.

Proof. Let $p^* = P_{F(T)}\bar{u}$. Then we have from (3.2), (2.1) and quasi-nonexpansiveness of T that

$$||u_{n+1} - p^*||^2 = ||\alpha_n \bar{u} + (1 - \alpha_n) T z_n + \eta_n - p^*||^2$$

$$= ||\alpha_n (\bar{u} - p^*) + \eta_n + (1 - \alpha_n) (T z_n - p^*)||^2$$

$$\leq (1 - \alpha_n) ||T z_n - p^*||^2 + 2||\eta_n|| ||u_{n+1} - p^*||$$

$$+ 2\alpha_n \langle \bar{u} - p^*, u_{n+1} - p^* \rangle$$

$$\leq (1 - \alpha_n) ||z_n - p^*||^2 + 2||\eta_n|| ||u_{n+1} - p^*||$$

$$+ 2\alpha_n \langle \bar{u} - p^*, u_{n+1} - p^* \rangle.$$
(3.12)

Again, we have from (3.2), (2.1), Lemma 2.1 and quasi-nonexpansiveness of T that

$$||z_{n} - p^{*}||^{2} = ||(1 - \lambda_{n})v_{n} + \lambda_{n}Tw_{n} + \sigma_{n} - p^{*}||^{2}$$

$$= ||(1 - \lambda_{n})(v_{n} - p^{*}) + \lambda_{n}(Tw_{n} - p^{*}) + \sigma_{n}||^{2}$$

$$\leq ||(1 - \lambda_{n})(v_{n} - p^{*}) + \lambda_{n}(Tw_{n} - p^{*})||^{2} + 2\langle\sigma_{n}, z_{n} - p^{*}\rangle$$

$$\leq (1 - \lambda_{n})||v_{n} - p^{*}||^{2} + \lambda_{n}||w_{n} - p^{*}||^{2}$$

$$- \lambda_{n}(1 - \lambda_{n})||Tw_{n} - v_{n}||^{2} + 2||\sigma_{n}|| ||z_{n} - p^{*}||.$$
(3.13)

From (3.2), (2.1) and the Cauchy Schwarz Inequality, we obtain

$$||v_{n} - p^{*}||^{2} = ||u_{n} + \theta_{n}(u_{n} - u_{n-1}) + \epsilon_{n} - p^{*}||^{2}$$

$$\leq ||u_{n} - p^{*}||^{2} + 2\langle \theta_{n}(u_{n} - u_{n-1}) + \epsilon_{n}, v_{n} - p^{*}\rangle$$

$$\leq ||u_{n} - p^{*}||^{2} + 2||\theta_{n}(u_{n} - u_{n-1}) + \epsilon_{n}|| ||v_{n} - p^{*}||.$$
(3.14)

Similarly, we obtain that

$$||w_n - p^*||^2 \le ||u_n - p^*||^2 + 2||\phi_n(u_n - u_{n-1}) + \rho_n|||w_n - p^*||.$$
(3.15)

Combination of (3.13), (3.14) and (3.15) gives

$$||z_{n} - p^{*}||^{2} \leq (1 - \lambda_{n}) [||u_{n} - p^{*}||^{2} + 2||\theta_{n}(u_{n} - u_{n-1}) + \epsilon_{n}||||v_{n} - p^{*}||]$$

$$+ \lambda_{n} [||u_{n} - p^{*}||^{2} + 2||\phi_{n}(u_{n} - u_{n-1}) + \rho_{n}||||w_{n} - p^{*}||]$$

$$+ 2||\sigma_{n}||||z_{n} - p^{*}|| - \lambda_{n}(1 - \lambda_{n})||Tw_{n} - v_{n}||^{2}$$

$$\leq ||u_{n} - p^{*}||^{2} + 2||\theta_{n}(u_{n} - u_{n-1}) + \epsilon_{n}||||v_{n} - p^{*}||$$

$$+ 2||\phi_{n}(u_{n} - u_{n-1}) + \rho_{n}|||w_{n} - p^{*}||$$

$$+ 2||\sigma_{n}||||z_{n} - p^{*}|| - \lambda_{n}(1 - \lambda_{n})||Tw_{n} - v_{n}||^{2}.$$

$$(3.16)$$

Substituting (3.16) into (3.12), we obtain

$$||u_{n+1} - p^*||^2 \le (1 - \alpha_n)||u_n - p^*||^2 + 2||\theta_n(u_n - u_{n-1}) + \epsilon_n||||v_n - p^*|| + 2||\phi_n(u_n - u_{n-1}) + \rho_n||||w_n - p^*|| + 2||\sigma_n||||z_n - p^*|| + 2||\eta_n||||u_{n+1} - p^*|| + 2\alpha_n\langle \bar{u} - p^*, u_{n+1} - p^*\rangle - (1 - \alpha_n)\lambda_n(1 - \lambda_n)||Tw_n - v_n||^2.$$

$$(3.17)$$

Denote $\Omega_n = ||u_n - p^*||^2$ and

$$\Delta_n = \frac{2}{\alpha_n} \|\theta_n(u_n - u_{n-1}) + \epsilon_n \|\|v_n - p^*\| + \frac{2}{\alpha_n} \|\phi_n(u_n - u_{n-1}) + \rho_n \|\|w_n - p^*\| + \frac{2}{\alpha_n} \|\sigma_n\|\|z_n - p^*\| + \frac{2}{\alpha_n} \|\eta_n\|\|u_{n+1} - p^*\| + 2\langle \bar{u} - p^*, u_{n+1} - p^* \rangle.$$

Using these notations and disregarding the last term of (3.17) we get

$$\Omega_{n+1} \le (1 - \alpha_n)\Omega_n + \alpha_n \Delta_n. \tag{3.18}$$

Moreover, rearranging (3.17) gives

$$(1 - \alpha_n)\lambda_n(1 - \lambda_n)\|Tw_n - v_n\|^2 \le \Omega_n - \Omega_{n+1} + \alpha_n(\Delta_n - \Omega_n). \tag{3.19}$$

To show that the sequence $\{\Omega_n\}$ of real numbers converges strongly to zero, we consider two cases.

Case I. Suppose there exists $N \in \mathbb{N}$ such that $\Omega_{n+1} \leq \Omega_n$ for all $n \geq N$. Then $\{\Omega_n\}$ is convergent. Thus, we obtain from (3.19) and the conditions on α_n and λ_n that

$$\lim_{n \to \infty} ||Tw_n - v_n|| = 0. \tag{3.20}$$

Moreover, we have

$$||Tw_n - w_n|| \le ||v_n - w_n|| + ||Tw_n - v_n|| \le ||Tw_n - v_n|| + ||\theta_n - \phi_n|||u_n - u_{n-1}|| + ||\epsilon_n - \rho_n||.$$
(3.21)

From (3.4), (3.20) and the conditions on ϵ_n and ρ_n , we have that limit as $n \to \infty$ of the right hand side of (3.21) is zero. Thus, it follows by the Squeezing Theorem that

$$\lim_{n \to \infty} ||Tw_n - w_n|| = 0. \tag{3.22}$$

Since $\{u_n\}$ is bounded, there exists a subsequence $\{u_{n_k}\}$ of $\{u_n\}$ such that $u_{n_k} \rightharpoonup \mathring{u}$ as $k \to \infty$ and

$$\limsup_{n \to \infty} \langle \bar{u} - p^*, \ u_n - p^* \rangle = \lim_{k \to \infty} \langle \bar{u} - p^*, \ u_{n_k} - p^* \rangle. \tag{3.23}$$

Since $\lim_{k\to\infty} ||w_{n_k} - u_{n_k}|| = 0$, one concludes that $w_{n_k} \to \mathring{u}$. Thus, we obtain from (3.21) and the demiclosedness property of I - T that $\mathring{u} \in F(T)$.

Since $p^* = P_{F(T)}\bar{u}$, we have from (2.3) and (3.23) that

$$\lim \sup_{n \to \infty} \langle \bar{u} - p^*, \ u_n - p^* \rangle = \lim_{k \to \infty} \langle \bar{u} - p^*, \ u_{n_k} - p^* \rangle = \langle \bar{u} - p^*, \ \mathring{u} - p^* \rangle \le 0, \ (3.24)$$

and this implies that

$$\limsup_{n \to \infty} \langle \bar{u} - p^*, \ u_{n+1} - p^* \rangle \le 0. \tag{3.25}$$

Thus, we conclude from (3.3), boundedness of $\{u_n\}$ $\{v_n\}$, $\{w_n\}$, $\{z_n\}$ and (3.25) that $\limsup_{n\to\infty} \Delta_n \leq 0$, and hence it follows by (3.18) and Lemma 2.3 that $\lim_{n\to\infty} \Omega_n = 0$, which implies that $\lim_{n\to\infty} \|u_n - p^*\| = 0$, that is, $u_n \to p^*$ as $n \to \infty$.

Case II. Suppose that there exists a subsequence $\{\Omega_{n_i}\}$ of $\{\Omega_n\}$ such that $\Omega_{n_i} < \Omega_{n_i+1}$, for all $i \geq 0$. Then, by Lemma 2.2, there exists a non-decreasing sequence $\{m_k\}$ of positive integers such that $\lim_{k\to\infty} m_k = \infty$ and

$$\Omega_{m_k} \le \Omega_{m_k+1} \text{ and } \Omega_k \le \Omega_{m_k+1},$$
(3.26)



for all positive integers k. In this case, relation (3.19) takes the form

$$(1 - \alpha_{m_k})\lambda_{m_k}(1 - \lambda_{m_k})\|Tw_{m_k} - v_{m_k}\|^2 \le \Omega_{m_k} - \Omega_{m_k+1} + \alpha_{m_k}(\Delta_{m_k} - \Omega_{m_k}). \quad (3.27)$$

Taking the limit of (3.27) and taking (3.26) and the properties of α_{m_k} and λ_{m_k} into account, we get $\lim_{k\to\infty} ||Tw_{m_k} - v_{m_k}|| = 0$. Using the same techniques as in Case I, we obtain

$$\limsup_{k \to \infty} \Delta_{m_k} \le 0.$$
(3.28)

Thus, we obtain from (3.18) and (3.26) that

$$\alpha_{m_k}\Omega_{m_k} \leq \Omega_{m_k} - \Omega_{m_k+1} + \alpha_{m_k}\Delta_{m_k} \leq \alpha_{m_k}\Delta_{m_k}$$

which implies that

$$\Omega_{m_k} \le \Delta_{m_k}. \tag{3.29}$$

Taking the limit of (3.29) and using (3.28), we get $\lim_{k\to\infty} \Omega_{m_k} = 0$ and hence $\lim_{k\to\infty} \Omega_{m_k+1} = 0$. Thus, it follows from (3.26) that $\lim_{k\to\infty} \Omega_k = 0$, and this in turn implies that $\lim_{k\to\infty} \|u_k - p^*\| = 0$ and hence the proof is complete.

The following are direct consequences of our main theorem.

Corollary 3.4. Let the conditions (C2) - (C5) hold and $T: \mathbb{H} \to \mathbb{H}$ be a nonexpansive mapping with $F(T) \neq \emptyset$. Then the sequence $\{u_n\}$ generated by Algorithm 3.1 converges strongly to p^* , where $p^* = P_{F(T)}\bar{u}$.

Corollary 3.5. Let the conditions (C2)-(C5) hold and $T: \mathbb{H} \to \mathbb{H}$ be a quasi-contractive mapping. Then the sequence $\{u_n\}$ generated by Algorithm 3.1 converges strongly to the unique fixed point of T.

If $\epsilon_n = \rho_n = \sigma_n = \eta_n = 0$, then Algorithm 3.1 reduces to its non-perturbed version and we obtain the following corollary.

Corollary 3.6. Let conditions (C1) - (C5) with $\epsilon_n = \rho_n = \sigma_n = \eta_n = 0$, for all $n \ge 1$ hold. Then the sequence $\{u_n\}$ generated by Algorithm 3.1 converges strongly to p^* , where $p^* = P_{F(T)}\bar{u}$.

Many other consequences can also be drawn by letting some of the inertial and perturbation parameters to be zero, while the others are kept to be nonzero.

4. Numerical example

In this section, we provide a quasi-nonexpansive mapping that is not nonexpansive and experimentally validate our theoretical results.

Example 4.1. Let $\mathbb{H} = \mathbb{R}$ with the usual norm and $T: \mathbb{R} \to \mathbb{R}$ be the mapping defined by

$$Tu = \begin{cases} \frac{u}{2} \cos\left(\frac{1}{u}\right) & \text{if } u \neq 0, \\ 0 & \text{otherwise.} \end{cases}$$

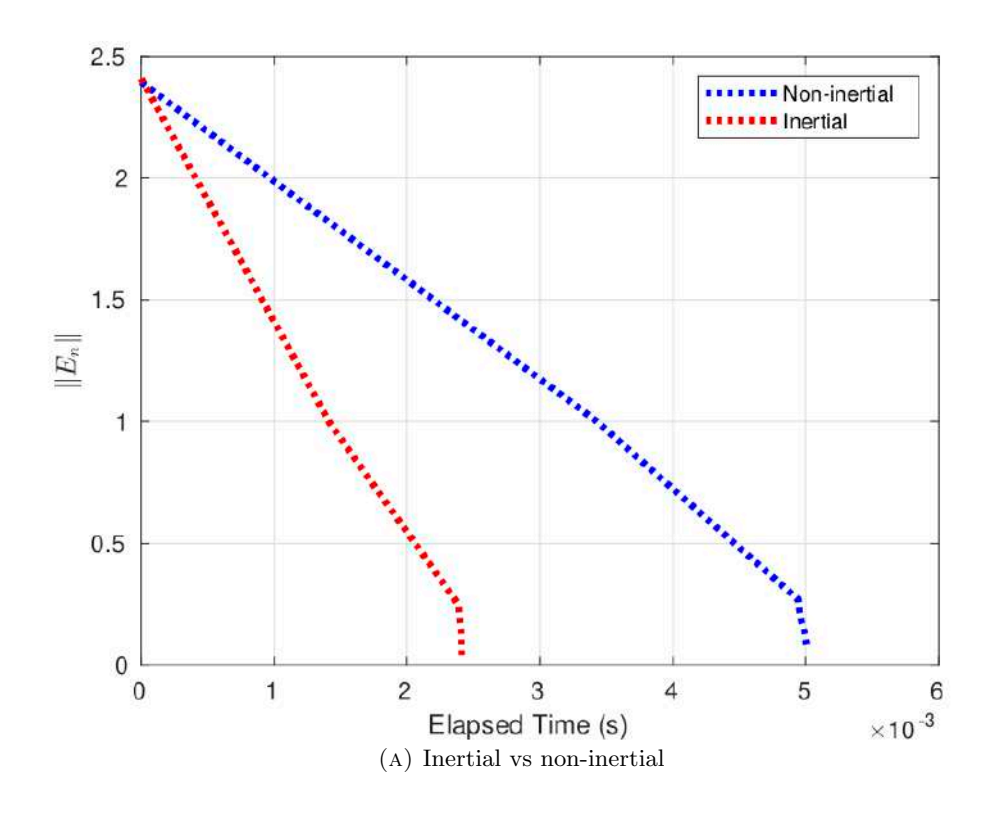
Then T is quasi-nonexpansive with $F(T) = \{0\}$, but it is not nonexpansive. To see this, we have for all $u \in (-\infty, 0) \cup (0, \infty)$ that

$$|Tu - 0| = \left| \frac{u}{2} \cos\left(\frac{1}{u}\right) - 0 \right| \le \frac{1}{2} \left| u - 0 \right| < |u - 0|.$$

However, if we take $u = \frac{1}{\pi}$ and $v = \frac{1}{2\pi}$. Then we get

$$|Tu - Tv| = \left|\frac{1}{2\pi}\cos(\pi) - \frac{1}{4\pi}\cos(2\pi)\right| = \frac{3}{4\pi}.$$

But, $|u-v|=\left|\frac{1}{\pi}-\frac{1}{2\pi}\right|=\frac{1}{2\pi}<\frac{3}{4\pi}$. Thus, T is not nonexpansive. Moreover, we have conducted a numerical experiment for this example using MATLAB programming and we obtained the following results. We took $\zeta_n=\frac{1}{n^2+10},\,\alpha_n=\frac{1}{n+10},$ $\epsilon_n = \frac{1}{n^2 + 2}, \, \rho_n = \frac{1}{n^2 + 2}, \, \sigma_n = \frac{1}{n^2 + 2}, \, \eta_n = \frac{1}{n^2 + 2}, \, \lambda_n = \frac{1}{n + 2} + \frac{1}{5}, \, \bar{u} = 0.1 \text{ and } p^* = 0.1$ 0. Thus, conditions (C1) - (C5) of Algorithm 3.1 are satisfied. We obtained the following graphs which demonstrate that the norm of the error term sequence $E_n = \{u_n - p^*\}$, $n \geq 1$, decreases and it converges to zero for the initial points $x_0 = 2$, $x_1 = 6$, $\alpha = 0.9$ and different perturbation and inertial parameters.



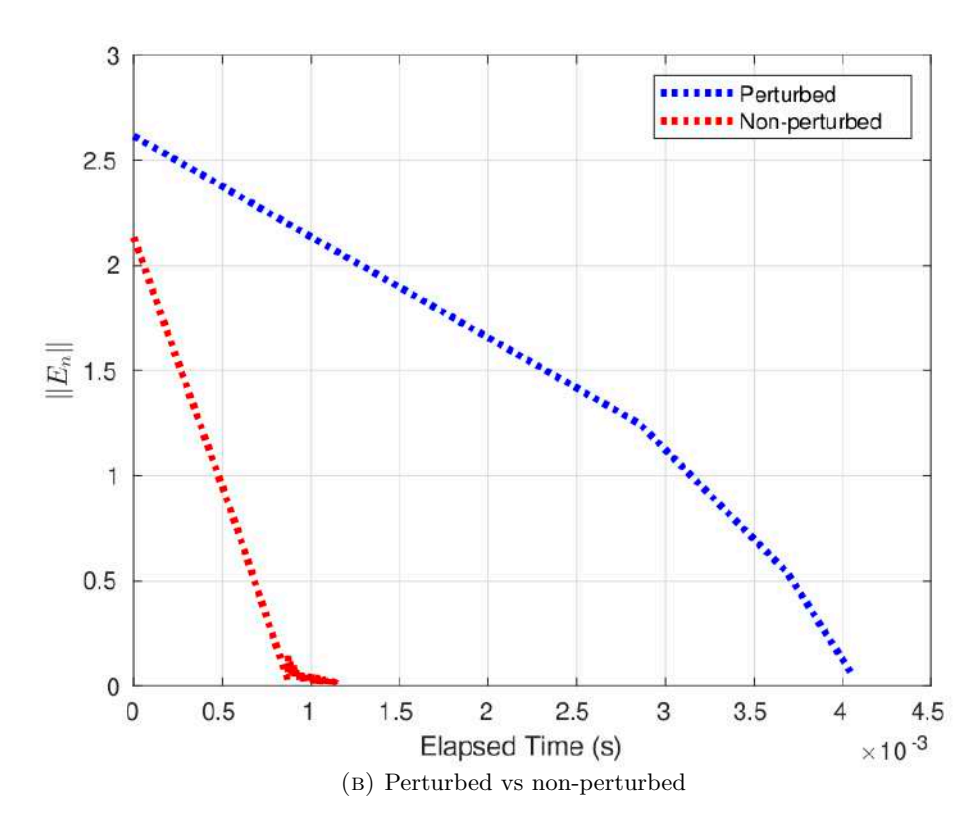


FIGURE 1. Convergence of Algorithm 3.1 for different values of the inertial and perturbation parameters.

Remark 4.2. Figure 1 depicts convergence of the method for different inertial and perturbation parameters. Particularly, sub-figure (A) shows that the inertial method ($\alpha \neq 0$) of Algorithm 3.1 converges at a faster rate than the non-inertial method ($\alpha = 0$). It can also be observed from sub-figure (B) that convergence of the non-perturbed version ($\epsilon_n = \rho_n = \sigma_n = \eta_n = 0$) of the algorithm is faster than that of the perturbed version. Though the perturbation parameters influence how quickly the method converges, they do not affect the algorithm ultimate convergence, indicating that the method remains stable under certain perturbations.

In addition to this, we have conducted comparison of the method introduced in this paper with the results of [5], [9] and [20]. Since the mapping considered in [5] is a quasi-contraction mapping, we took $Tx = \frac{x}{2}$ for the comparison case, keeping all other parameters the same as that of Example 4.1.

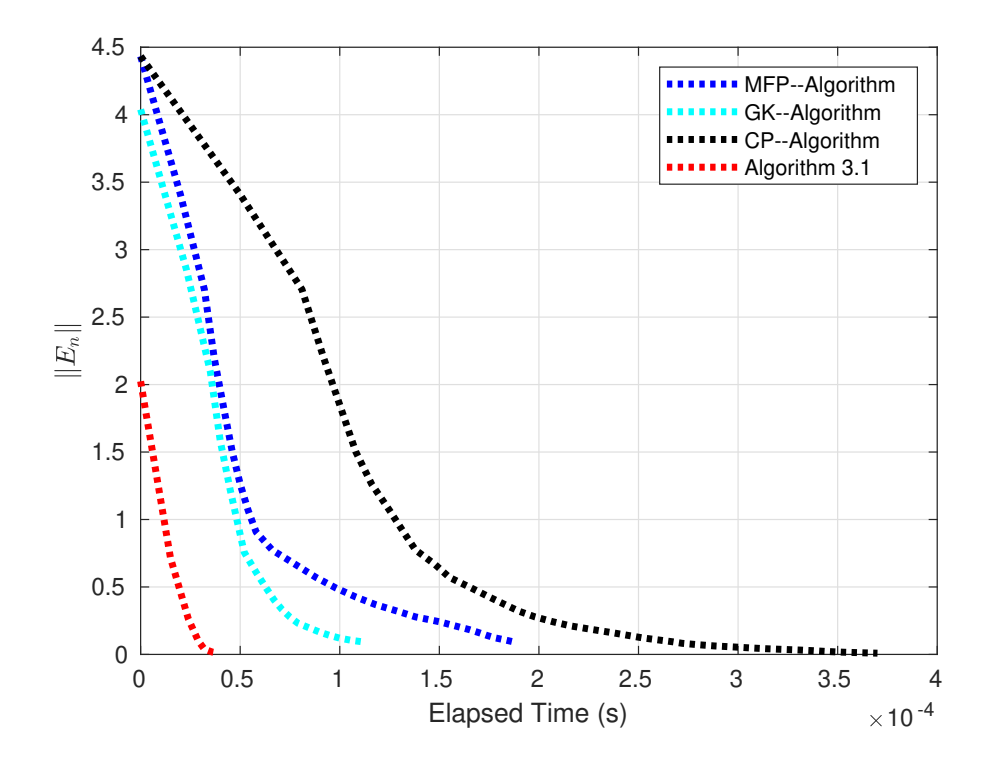


FIGURE 2. Comparison of convergence rates with results in the literature.

Remark 4.3. Figure 2 shows the comparison between Algorithm 3.1 of this paper and the main algorithms in Cortild and Peypouquet [5] (labeled as CP-Algorithm), Gebregiorgis and Kumam [9] (labeled as GK-Algorithm), and Maulen, Fierro and Peypouquet [20] (labeled MFP-Algorithm). The fact that our method converges considerably more quickly than other approaches in the literature indicates that our approach works more effectively.

5. Applications to image restoration problems

Image deblurring refers to the restoration of sharpness and fine details in an image by mitigating the effects of blur introduced by different factors such as camera shake, subject movement, de-focused lenses, or environmental conditions such as low light or wind. Image deblurring is an inherent inverse problem, where the goal is to reverse the effects of the blurring process, and it is an important problem in the field of image processing.

The concept of image deblurring is to restore an original image u from the degraded image ν . The images $u \in \mathbb{R}^{n \times 1}$ and $\nu \in \mathbb{R}^{m \times 1}$ are related by the mathematical model

$$\nu = \Delta u + \omega$$
,

where $\Delta \in \mathbb{R}^{m \times n}$ is a blur operator and $\omega \in \mathbb{R}^{m \times 1}$ is noise. To find the restored image, we can solve the following optimization problem:



find
$$u \in \operatorname{argmin}_{u \in \mathbb{R}^{n \times 1}} \left\{ \frac{1}{2} \|\Delta u - \nu\|_2^2 + \tau \|u\|_1 \right\},$$
 (5.1)

where τ is the regularization parameter, $\|\cdot\|_1$ is the l_1 norm and $\|\cdot\|_2$ is the usual norm. If we let $f(u) = \frac{1}{2} \|\Delta u - \nu\|^2$ and $g(u) = \tau \|u\|_1$, then solving (5.1) is equivalent to solving the monotone inclusion problem of

finding
$$u \in \mathbb{R}^{n \times 1}$$
 such that $0 \in (A+B)u$, (5.2)

with $A = \nabla f$ and $B = \partial g$, where ∂g is the sub-differential of g, that is, $\partial g(x) = \{v \in \mathbb{R}^n : g(y) \geq g(x) + \langle v, y - x \rangle$, for all $y \in \mathbb{R}^n\}$ and ∇f is the gradient of f. We recall that ∇f is monotone and ∂g is maximally monotone. For further knowledge of inclusion problems and their applications in image restoration, one can refer (for instance, [1, 29, 30, 41] and references therein). Solving (5.2), in turn, is equivalent to finding the fixed point of the mapping

$$T_{r_n} = (I + r_n B)^{-1} (I - r_n A), (5.3)$$

for $r_n > 0$ (see, Lemma 2.4), provided that the set of solutions of (5.2) is nonempty. For the image restoration, we begun by selecting clear original mandrill and butterfly images. Then we applied four different types of blurring on each image, namely the average blur, disk blur, Gaussian blur, and motion blur to get some degraded images. Then we recovered the resulting blurred images. We also analyze the Structural Similarity Index Measure (SSIM) and Improvement in the Signal-to-Noise Ratio (ISNR) to evaluate the quality of the deblurred images and effectiveness of the deblurring method we employed. For these aforementioned image quality measures, we used the formulas

$$SSIM(u, u_n) = \frac{(2\mu_u \mu_{u_n} + C_1)(2\sigma_{uu_n} + C_2)}{(\mu_u^2 + \mu_{u_n}^2 + C_1)(\sigma_u^2 + \sigma_{u_n}^2 + C_2)}, \text{ and}$$

$$ISNR(n) = 10 \log_{10} \left(\frac{\|u - \nu\|_2^2}{\|u - u_n\|_2^2} \right),$$

where u, ν and u_n are the original clean image, the blurred image, and the recovered image, respectively; μ_u and μ_{u_n} are intensities of the images u and u_n , respectively; σ_u^2 and $\sigma_{u_n}^2$ are the variances of u and u_n , respectively; σ_{uu_n} is the covariance between u and u_n ; $C_1 = (\kappa_1 L)^2$, $C_2 = (\kappa_2 L)^2$ are stabilization constants with the default constants κ_1 and κ_2 (set in our bese to be $\kappa_1 = 0.01$ and $\kappa_2 = 0.03$) and L is the dynamic range of pixel values (in our case, we took L = 255). In our experimentation, we employed different parameters for the different types of blurs. The outcomes of the conducted experiments for n = 3000 iterations, regularization parameter $\tau = 0.001$, $r_n = 0.5 - \frac{150n}{1000n + 100}$, average blur of kernel 15×15 matrix, disk blur with radius of blur r = 6 pixels, Gaussian blur with standard deviation $\sigma = 3$ pixels, and motion blur of length l = 9 pixels, are depicted in Figures 3 through 10 below.

Moreover, we have tried to compare the quality of images restored by our algorithm and the main algorithm of [9] against the aforementioned SSIM and ISNR metrics using different parameters for each type of blur.

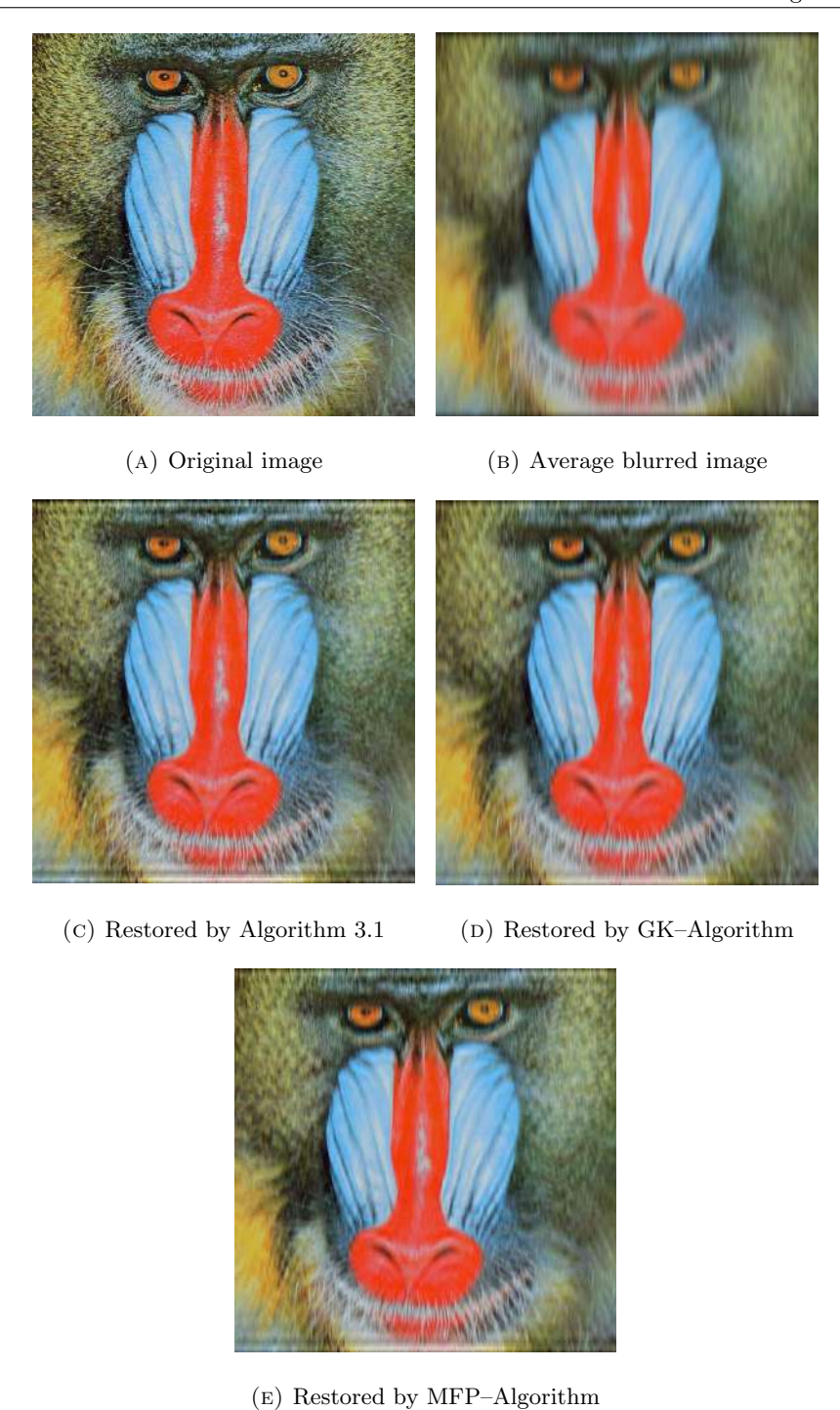


FIGURE 3. Original and average blurred images of a mandrill along with the restored images by Algorithm 3.1, GK–Algorithm and MFP–Algorithm, respectively.

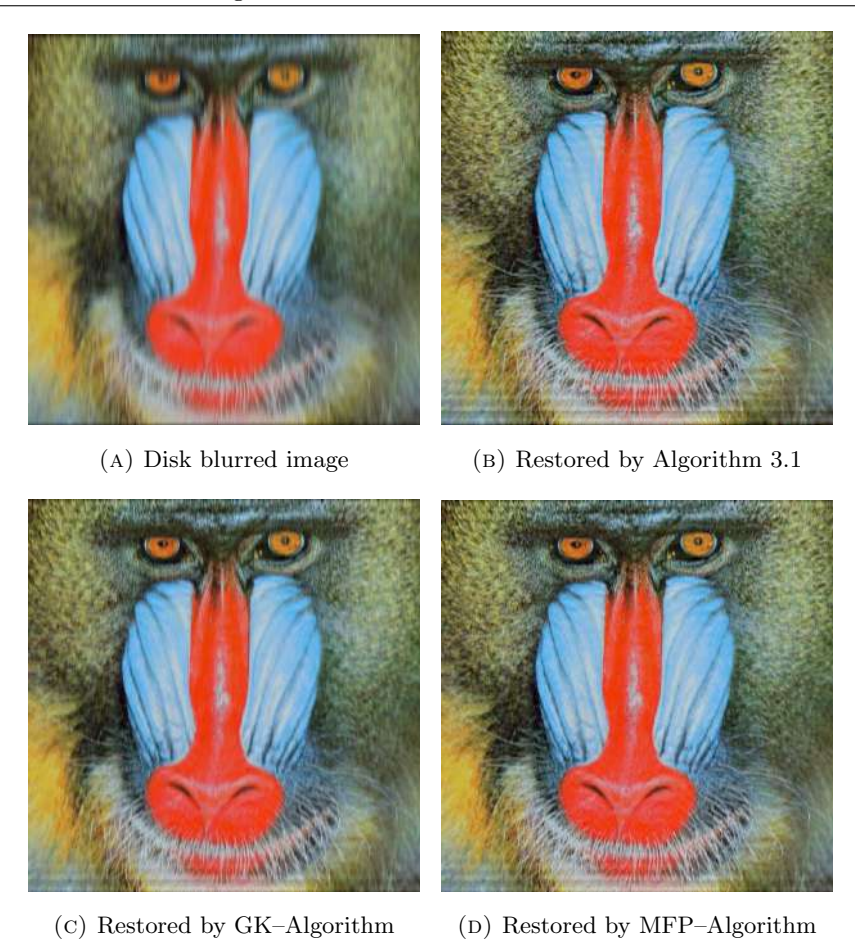
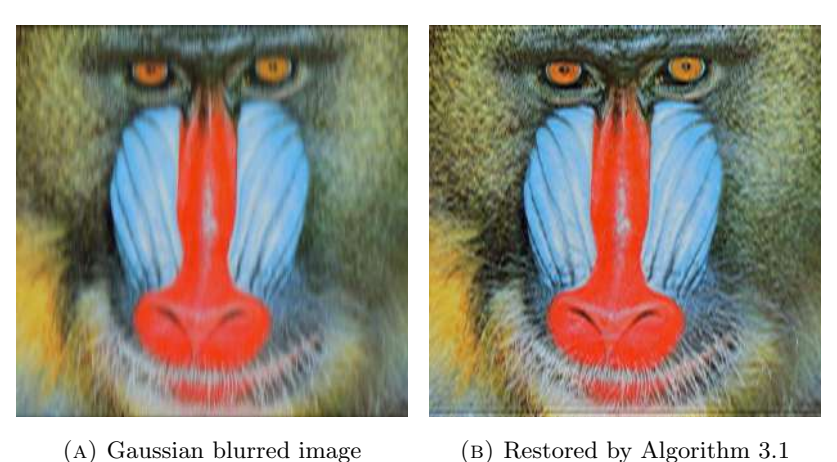
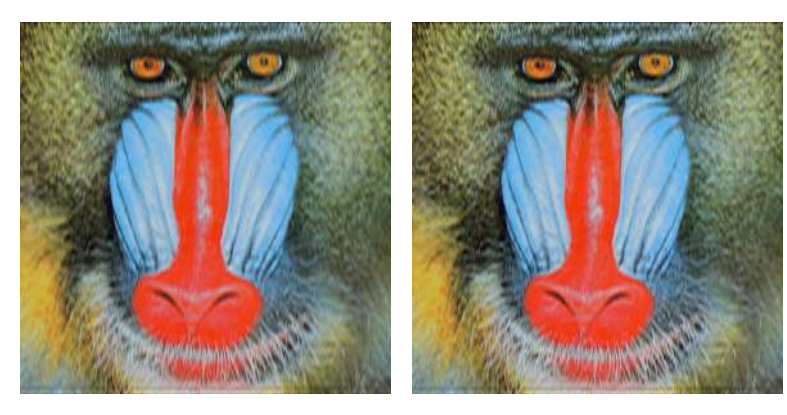


FIGURE 4. Disk blurred image of a mandrill along with the restored images by Algorithm 3.1, GK-Algorithm and MFP-Algorithm, respectively.

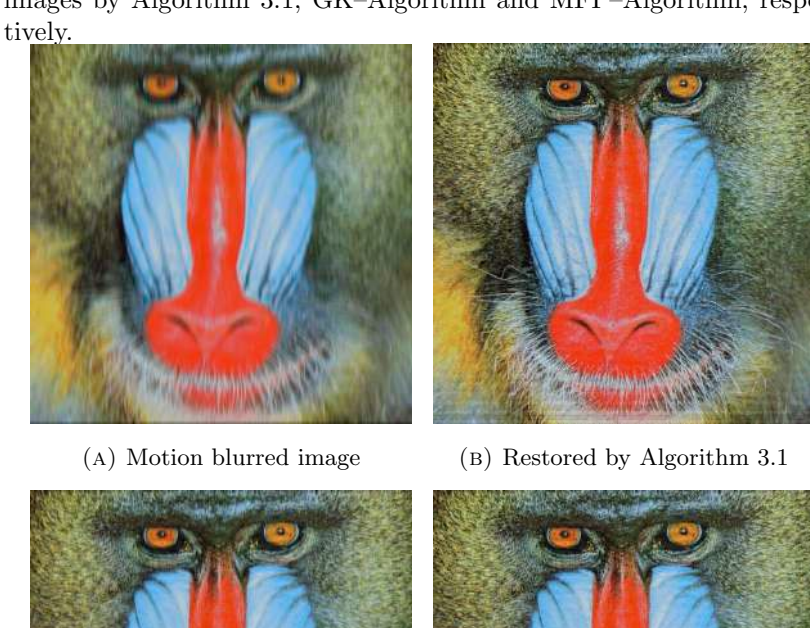


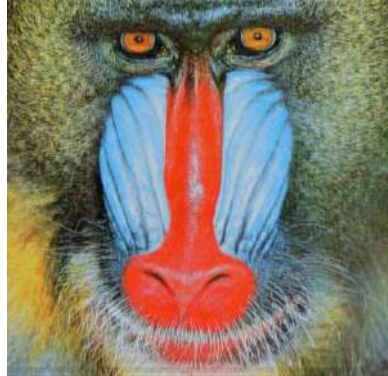


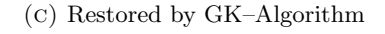
(c) Restored by GK-Algorithm

(D) Restored by MFP-Algorithm

FIGURE 5. Gaussian blurred image of a mandrill along with the restored images by Algorithm 3.1, GK-Algorithm and MFP-Algorithm, respectively







(D) Restored by MFP-Algorithm

FIGURE 6. Original and motion blurred image of a mandrill along with the restored images by Algorithm 3.1, GK–Algorithm and MFP–Algorithm, respectively.

Table 1. Performance comparison, in terms of ISNR and SSIM, between Algorithm 3.1, the GK–Algorithm and MFP–Algorithm for various blurring methods applied to the mandrill images.

Method used Type of blur	Algorithm 3.1		GK-Al	gorithm	MFP-Algorithm		
	ISNR	SSIM	ISNR	SSIM	ISNR	SSIM	
Average blur (Kernel= 5×5)	4.4579	0.8881	1.8248	0.7214	2.7755	0.7807	
Disk blur $(r = 2 \text{ pxl})$	7.6840	0.9386	3.7865	0.8480	5.6274	0.9024	
Gaussian blur ($\sigma = 0.1 \text{ pxl}$)	6.3848	0.9710	5.0097	0.9569	6.2000	0.9672	
Motion blur $(l = 3 \text{ pxl})$	8.7536	0.9613	4.5405	0.9039	6.3030	0.9359	

Remark 5.1. In Figure 3, image 3(A) is the original clean image of the mandrill, image 3(B) is the image obtained by imposing average blur on image 3(A) while 3(C), 3(D) 3(E) reveal the images obtained by deblurring image 3(B) using Algorithm 3.1, the main Algorithm of [9] and that of [20], respectively.

Similarly, the images in Figures 4, 5, 6 reveal the disk, Gaussian and motion blurred images, respectively, of the the mandrill image along with respective deblurred images.

In order to clearly observe the resemblance of the restored images in Figures 3–6 with the original image, we have tried to analyze the SSIM and ISNR metrics for each restored image under each blur type. Table 1 shows the detailed comparison of ISNR and SSIM of Alg. 3.1 and the main algorithms of [9] and [20] for the four types of blurs applied on the clean original image. It can also be observed from these table that our method has relatively better performance than that of [9] and [20]. It can also be seen from Table 1 that the proposed method exhibits superior performance in handling motion blur, surpassing other evaluated blur types.

Table 2. Comparison of Algorithm 3.1, GK-Algorithm and MFP-Algorithm using motion blur with different blur lengths applied on the mandrill image.

Method used Length of blur	Algorithm 3.1		GK-Algorithm		MFP-Algorithm	
	ISNR	SSIM	ISNR	SSIM	ISNR	SSIM
l=3 pixels	8.7536	0.9613	4.5405	0.9039	6.3030	0.9359
l=9 pixels	7.4527	0.8943	3.9074	0.7584	5.5413	0.8371
l = 12 pixels	7.6528	0.8925	3.6607	0.7156	5.3692	0.8143
l = 15 pixels	6.7280	0.8584	3.3554	0.6680	4.7454	0.7669
l = 18 pixels	5.8790	0.8085	3.1737	0.6260	4.3037	0.7163
l=21 pixels	4.9106	0.7494	2.8157	0.5720	3.6668	0.6532

Method used Radius of disk blur	Algorithm 3.1		GK-Algorithm		MFP-Algorithm	
	ISNR	SSIM	ISNR	SSIM	ISNR	SSIM
r=2 pixels	7.6840	0.9386	3.7865	0.8480	5.6271	0.9024
r=4 pixels	5.2155	0.8335	2.6309	0.6834	3.6459	0.7531
r=6 pixels	3.7361	0.7307	2.0233	0.5760	2.7337	0.6640
r=8 pixels	2.9529	0.6360	1.7723	0.5047	2.3115	0.5632
r = 10 pixels	2.6376	0.5879	1.6275	0.4588	2.0908	0.5121
r = 15 pixels	2.3051	0.4903	1.6089	0.3880	1.9672	0.4287

TABLE 3. Comparison of Alg. 3.1, GK-Alg. and MFP – Alg for disk blur with different radii applied on the mandrill image.

Remark 5.2. In motion blur, as the length of the blur increases in image restoration problems, the restoration process becomes more challenging due to the multiple effects of information loss, noise amplification, difficulties in point spread function (PSF) estimation, increased computational demands, and perceptual limitations and this is complemented by the of the ISNR and SSIM values in Table 2. Similarly, as shown in Table 3, increasing the blur radius in a motion blur leads to a decline in the effectiveness of the restoration process.

In order to show the consistence of our method, we have conducted a similar experiment for a butterfly image. The resulting blurred and restored images can be seen in Figures 7-10 below.



(A) Original butterfly image



(B) Average blurred image





(c) Restored by Algorithm 3.1

(D) Restored by GK–Algorithm



(E) Restored by MFP-Algorithm

FIGURE 7. Original butterfly and average blurred images of a butterfly along with the restored images by Algorithm 3.1, GK–Algorithm and MFP–Algorithm, respectively.



(A) Disk blurred image



(B) Restored by Algorithm 3.1.







(C) Restored by GK–Algorithm

(D) Restored by MFP-Algorithm

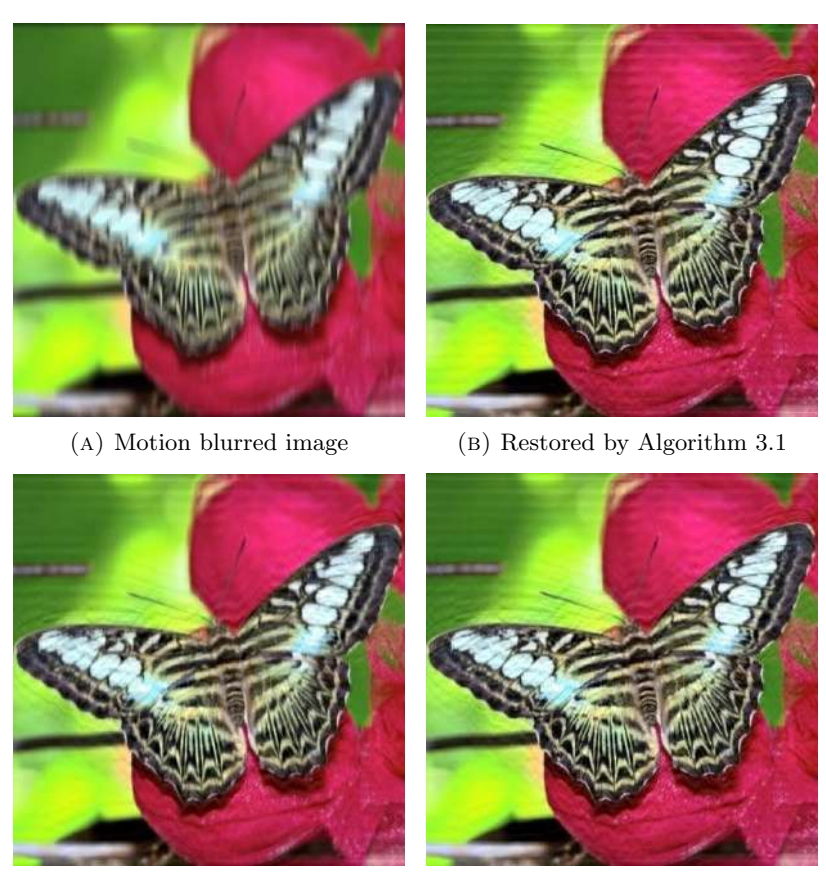
FIGURE 8. Disk blurred image of a butterfly along with the restored images by Algorithm 3.1, GK–Algorithm and MFP–Algorithm, respectively.



(c) Restored by GK-Algorithm

(D) Restored by MFP-Algorithm

FIGURE 9. Gaussian blurred image of a butterfly along with the restored images by Algorithm 3.1, GK–Algorithm and MFP–Algorithm, respectively



(c) Restored by GK-Algorithm

(D) Restored by MFP-Algorithm

FIGURE 10. Motion blurred image of a butterfly along with the restored images by Algorithm 3.1, GK–Algorithm and MFP–Algorithm, respectively.

Table 4. Comparison, in terms of ISNR and SSIM, between Algorithm 3.1, the GK-Algorithm and MFP-Algorithm for various blurring methods applied to the butterfly images.

Method used Type of blur	Algorithm 3.1		GK-Algorithm		MFP-Algorithm	
	ISNR	SSIM	ISNR	SSIM	ISNR	SSIM
Average blur (Kernel= 15×15)	3.9005	0.7698	2.6141	0.7417	3.4038	0.7604
Disk blur $(r = 9 \text{ pxl})$	6.8749	0.8093	4.0822	0.7684	5.4988	0.7907
Gaussian blur ($\sigma = 3$ pxl)	4.6463	0.8603	3.8232	0.8439	4.4781	0.8556
Motion blur $(l = 12 \text{ pxl})$	10.1697	0.8904	6.3055	0.8653	8.3077	0.8824

Table 5. Initial SSIM and ISNR measurements of Algorithm 3.1 for the Mandrill and Butterfly images that were deteriorated by different types of blur.

Blur type	Blurring parameters	Man	drill	Butterfly	
Blur type	Biurring parameters	ISNR	SSIM	ISNR	SSIM
Average	averaging filter = 18	0	0.4650	0	0.7352
Disk	radius = 12	0	0.5465	0	0.7807
Gaussian	Gaussian blur kernel = 20, standard deviation $(\sigma) = 6$	0	0.4138	0	0.7208
Motion	pixels length = 15 , degrees angle = 40	0	0.8589	0	0.8692

Remark 5.3. Figure 7 Sub-figure (A) displays the original, unaltered butterfly image. Sub-figure (B) illustrates the image after the application of average blur. Sub-figures (C), (D) and (E) depict the results of deblurring the blurred image in sub-figure (B) using Algorithm 3.1, GK-Algorithm [9] and MFP-Algorithm [20], respectively.

Similarly, Figures 8, 9, and 10 showcase the effects of disk blur, Gaussian blur, and motion blur, respectively, on the "butterfly" image. Each figure includes the blurred image alongside the corresponding deblurred output obtained by Algorithm 3.1, GK-Algorithm [9], and MFP-Algorithm [20].

Table 4 provides a quantitative comparison of the ISNR and SSIM metrics for both Algorithm 3.1 and the main algorithm in [9] and [20] across all the four types of blur. The results indicate that Algorithm 3.1 consistently performs better than the results in [9] and [20], with particularly notable improvements observed in the motion blur scenario since higher ISNR value corresponds to the better quality of the restored image.

It can generally be observed from Tables 1, 4, and 5 that the values of the SSIMs of the restored images are far better than the degraded images for all blur types applied on both the Mandrill and the Butterfly images.

6. Conclusions

An inertial Halpern-type approach for approximating solutions of perturbed Krasnoselskii–Mann iterations was presented in this paper. We discussed the strong convergence analysis under the assumption that the underlying mapping is quasi–nonexpansive. A numerical example was provided to demonstrate the practicality of our method. Furthermore, we have explored the application of the method in image restoration problems, specifically addressing cases involving Average blur, Disk blur, Gaussian blur, and motion blur applied on Mandrill and Butterfly images.

To assess the efficiency of our proposed image restoration algorithm application, we conducted a comparison focusing on the two key performance metrics: the ISNR and SSIM. These metrics were evaluated against those obtained from the algorithms presented in [9] and [20]. Our findings from ISNR and SSIM metrics indicate that our method achieves superior performance in both metrics, suggesting a more effective restoration capability compared to the referenced methods. Generally, the result in this work extends several existing results in the literature in various directions. Specifically, it generalizes the finding of [5], where the mapping considered in their strong convergence theorem is quasicontractive, while in our case it is quasi-nonexpansive a broader class than contractive mappings. In addition to this, our method dispenses the assumption that the perturbation



parameters are summable, which is a requirement for the strong convergence in [5]. In addition, our result improves upon that of [9] as the assumptions $\lim_{n\to\infty} \frac{\theta_n}{\alpha_n} ||u_n - u_{n-1}|| = 0$ and $\lim_{n\to\infty} \frac{\phi_n}{\alpha_n} ||u_n - u_{n-1}|| = 0$, which were required in their work, are not imposed as assumptions in our method because they follow directly from (3.1). As such, our result generalizes and strengthens several related results in the existing literature.

ACKNOWLEDGMENTS

The authors gratefully acknowledge the support provided by Naresuan University (NU) under the Global and Frontier Research University project, No. R2568C003. Moreover, This project and Kasamsuk Ungchittrakool are supported by National Research Council of Thailand (NRCT) and Naresuan University. Grant NO. N42A660516.

DECLARATIONS

Ethical approval: Not applicable.

Availability of supporting data: Not applicable.

Competing interests: The authors declare that there are no conflicts of interest.

Funding: The Global and Frontier Research University project, No. R2568C003. Moreover, This project and Kasamsuk Ungchittrakool are supported by National Research Council of Thailand (NRCT) and Naresuan University. Grant NO. N42A660516.

Authors' contributions: All authors worked equally on the results and approved the final manuscript.

References

- [1] A. Adamu, D. Kitkuan, T. Seangwattana, An accelerated Halpern-type algorithm for solving variational inclusion problems with applications, Bangmod International Journal of Mathematical and Computational Science 8 (2022) 37–55. Available from: https://doi.org/10.58715/bangmodjmcs.2022.8.4.
- [2] N. Artsawang, S. Plubtieng, O. Bagdasar, K. Ungchittrakool, S. Baiya, P. Thammasiri, Inertial Krasnoselski-Mann iterative algorithm with step-size parameters involving nonexpansive mappings with applications to solve image restoration problems, Carpathian Journal of Mathematics 40 (2024) 243–261. Available from: https://doi.org/10.37193/CJM.2024.02.02.
- [3] N. Artsawang, K. Ungchittrakool, Inertial Mann-type algorithm for a nonexpansive mapping to solve monotone inclusion and image restoration problems, Symmetry 12(5) (2020) 1–17. Available from: https://doi.org/10.3390/sym12050750.
- [4] A. Azam, J. Ahmad, P. Kumam, Common fixed point theorems for multi-valued mappings in complex-valued metric spaces, Journal of Inequalities and Applications 2013 (2013) 1–12. Available from: https://doi.org/10.1186/1029-242X-2013-578.
- [5] D. Cortild, J. Peypouquet, Krasnoselskii–Mann Iterations: Inertia, Perturbations and Approximation, Journal of Optimization Theory and Applications 204(2) (2025), 35. Available from: https://doi.org/10.1007/s10957-024-02600-5.

[6] P.L. Combettes, Solving monotone inclusions via compositions of nonexpansive averaged operators, Optimization 53(5–6) (2004) 475–504. Available from: https://doi.org/10.1080/02331930412331327157.

- [7] Q.L. Dong, Y.J. Cho, S. He, P.M. Pardalos, T.M. Rassias, The Krasnosel'ski-Mann Iterative Method: Recent Progress and Applications. Springer, 2022.
- [8] M. Edelstein, On nonexpansive mappings, Proceedings of the American Mathematical Society 15 (1964) 689–695.
- [9] S. Gebregiorgis, P. Kumam, Convergence results on the general inertial Mann–Halpern and general inertial Mann algorithms, Fixed Point Theory Algorithms for Science and Engineering 2023(1) (2023) 18. Available from: https://doi.org/10.1186/s13663-023-00752-z.
- [10] K. Goebel, W.A. Kirk, A fixed point theorem for asymptotically nonexpansive mappings, Proceedings of the American Mathematical Society 35(1) (1972) 171–174.
- [11] A. Inuwa, S.S. Musa, Approximation Method for Common Fixed Point of a Countable Family of Multi-valued Quasi-φ-Nonexpansive Mappings in Banach Spaces, Bangmod International Journal of Mathematical and Computational Science 9 (2023) 45–62. Available from: https://doi.org/10.58715/bangmodjmcs.2023.9.4.
- [12] O.S. Iyiola, Y. Shehu, New convergence results for inertial Krasnoselski-Mann iterations in Hilbert spaces with applications, Results in Mathematics 76(2) (2021) 75. Available from: https://doi.org/10.1007/s00025-021-01381-x.
- [13] J.N. Ezeora, C. Izuchukwu, A.A. Mebawondu, O.T. Mewomo, Approximating common fixed points of mean nonexpansive mappings in hyperbolic spaces, International Journal of Nonlinear Analysis and Applications 12(1) (2021) 231–244. Available from: http://dx.doi.org/10.22075/ijnaa.2021.4775.
- [14] C. Kanzow, Y. Shehu, Generalized Krasnoselskii–Mann–type iterations for nonexpansive mappings in Hilbert spaces, Computational Optimization and Applications 67(3) (2017) 593–620. Available from: https://doi.org/10.1007/s10589-017-9902-0.
- [15] M.A. Krasnosel'skii, Two remarks on the method of successive approximations, Uspekhi Matematicheskikh Nauk 10(63) (1955) 123–127.
- [16] P. Kumam, Fixed point theorems for nonexpansive mappings in modular spaces, Archivum mathematicum 40(4) (2004) 345–353.
- [17] Y. Lin, C.R. Schidtlein, Q. Li, S. Li, Y. Xu, A Krasnoselskii–Mann algorithm with an improved EM preconditioner for PET image reconstruction, IEEE TRANS-ACTIONS ON MEDICAL IMAGING 38(9) (2019) 2114–2126. https://doi.org/10.1109/TMI.2019.2898271.
- [18] P.E. Maingé, Strong convergence of projected subgradient methods for nonsmooth and nonstrictly convex minimization, Set–Valued Analysis 16 (2008), 899–912. Available from: https://doi.org/10.1007/s11228-008-0102-z.
- [19] W.R. Mann, Mean value methods in iteration, Proceedings of the American Mathematical Society 4 (1953), 506–510.
- [20] J.J. Maulén, I. Fierro, J. Peypouquet, Inertial krasnoselskii–mann iterations, Set–Valued and Variational Analysis, 32(2) (2024). Available from: https://doi.org/10.1007/s11228-024-00713-7.
- [21] A. Padcharoen, P. Kumam, P. Chaipunya, Y. Shehu, Convergence of inertial modified Krasnosel'skii-Mann iteration with application to image recovery, Thai Journal of Mathematics 18(1) (2020) 126–141.



- [22] A. Padcharoen, D. Kitkuan, W. Kumam, P. Kumam, Tseng methods with inertia for solving inclusion problems and application to image deblurring and image recovery problems, Computational and Mathematical Methods 3(3) (2021). Available from: https://doi.org/10.1002/cmm4.1088.
- [23] H. Piri, P. Kumam, Some fixed point theorems concerning F-contraction in complete metric spaces, Fixed Point Theory and Applications 2014(210) (2014). Available from: https://doi.org/10.1186/1687-1812-2014-210.
- [24] S. Reich, A.J. Zaslavski, Convergence of Krasnosel'skii-Mann iterations of nonexpansive operators, Mathematical and Computer Modeling 32(11–13) (2000) 1423–1431.
- [25] H.F. Senter, W.G. Dotson, Approximating fixed points of nonexpansive mappings, Proceedings of the American Mathematical Society 44(2) (1974) 375–380.
- [26] Y. Shehu, O.T. Mewomo, Further investigation into split common fixed point problem for demicontractive operators, Acta mathematica sinica, english series 32 (2016) 1357–1376. Available from: https://doi.org/10.1007/s10114-016-5548-6.
- [27] Y. Shehu, O.S. Iyiola, S. Reich, A modified inertial subgradient extragradient method for solving variational inequalities, Optimization and Engineering, 23(1) (2022) 421–449. Available from: https://doi.org/10.1007/s11081-020-09593-w.
- [28] C. Suanoom, B. Tanut, T. Grace, The Proposition for an CAK-Generalized Nonexpansive Mapping in Hilbert Spaces, Bangmod International Journal of Mathematical and Computational Science 8 (2022) 100–108. Available from: https://doi.org/10.58715/bangmodjmcs.2022.8.7.
- [29] P. Thammasiri, V. Berinde, N. Petrot, K. Ungchittrakool, Double Tseng's algorithm with inertial terms for inclusion problems and applications in image deblurring, Mathematics 12(19) (2024) 3138. Available from: https://doi.org/10.3390/math 12193138.
- [30] P. Thammasiri, R. Wangkeeree, K. Ungchittrakool, A modified inertial Tsengs algorithm with adaptive parameters for solving monotone inclusion problems with efficient applications to image deblurring problems, Journal of Computational Analysis and Applications 33(7) (2024) 782–797.
- [31] A.R. Tufa, H. Zegeye, Mann and Ishikawa-type iterative schemes for approximating fixed points of multi-valued non-self mappings, Mediterranean Journal of Mathematics 13 (2016), 4369–4384. Available from: https://doi.org/10.1007/s00009-016-0750-4.
- [32] G.C. Ugwunnadi, C. Izuchukwu and O.T. Mewomo, Proximal point algorithm involving fixed point of nonexpansive mapping in p-uniformly convex metric space, Advances in Pure and Applied Mathematics 10(4) (2019) 437–446. https://doi.org/10.1515/apam-2018-0026.
- [33] K. Ungchittrakool, S. Plubtieng, N. Artsawang, P. Thammasiri, Modified Mann-type algorithm for two countable families of nonexpansive mappings and application to monotone inclusion and image restoration problems, Mathematics 11 (2023) 2927. Available from: https://doi.org/10.3390/math11132927.
- [34] R. Wangkeeree, An iterative approximation method for a countable family of nonexpansive mappings in Hilbert spaces, Bulletin of the Malaysian Mathematical Sciences Society. Second Series 32(3) (2009) 313–320.
- [35] R. Wangkeeree, The General Hybrid Approximation Methods for Nonexpansive Mappings in Banach Spaces, Abstract and Applied Analysis 2011(1) (2011) 854360. Available from: https://doi.org/10.1155/2011/854360.

[36] R. Wangkeeree, N. Petrot, R. Wangkeeree, The general iterative methods for non-expansive mappings in Banach spaces, Journal of Global Optimization 51(1) (2011) 27–46. Available from: https://doi.org/10.1007/s10898-010-9617-6.

- [37] R. Wangkeeree, P. Preechasilp, Viscosity approximation methods for nonexpansive mappings in CAT(0) spaces, Journal of Inequalities and Applications 2013 (2013) 1–15. Available from: https://doi.org/10.1186/1029-242X-2013-93.
- [38] R. Wangkeeree, U. Boonkong, P. Preechasilp, Viscosity approximation methods for asymptotically nonexpansive mapping in CAT(0) spaces, Fixed Point Theory and Applications 2015 (2015) 1–15. Available from: https://doi.org/10.1186/s13663-015-0273-x.
- [39] H.K. Xu, Iterative algorithms for nonlinear operators, Journal of London Mathematical Society 66(1) (2002) 240–256. Available from: https://doi.org/10.1112/S00246 10702003332.
- [40] H.K. Xu, Viscosity approximation methods for nonexpansive mappings, Journal of Mathematical Analysis and Applications 298(1) (2004) 279–291. Available from: https://doi.org/10.1016/j.jmaa.2004.04.059.
- [41] P. Yodjai, P. Kumam, D. Kitkuan, W. Jirakitpuwapat, S. Plubtieng, The Halpern approximation of three operators splitting method for convex minimization problems with an application to image inpainting, Bangmod International Journal of Mathematical and Computational Science 5 (2019) 58–75.
- [42] H. Zegeye, N. Shahzad, Viscosity approximation methods for a common fixed point of finite family of nonexpansive mappings, Applied MAthematics and Computation 191(1) (2007) 155–163. Available from: https://doi.org/10.1016/j.amc.2007.02.072.
- [43] H. Zegeye, N. Shahzad, Convergence of Manns type iteration method for generalized asymptotically nonexpansive mappings, Computers & Mathematics with Applications 62(11) (2011) 4007–4014. Available from: https://doi.org/10.1016/j.camwa.2011.09.018.
- [44] H. Zegeye, N. Shahzad, Viscosity methods of approximation for a common fixed point of a family of quasi-nonexpansive mappings, Nonlinear Analysis: Theory, Methods & Applications 68(7) (2008) 2005–2012. Available from: https://doi.org/10.1016/j.na.2007.01.027.